PERGAMON

International Journal of Solids and Structures 38 (2001) 5149–5164

INTERNATIONAL JOURNAL OF SOLIDS and STRUCTURES

www.elsevier.com/locate/ijsolstr

A viscoelastic–viscoplastic constitutive model for glassy polymers

Geoffrey J. Frank *, Robert A. Brockman

University of Dayton, 300 College Park Avenue, Dayton, OH 45469-0110, USA

Received 7 April 1998

Abstract

A constitutive model is presented which combines nonlinear viscoelasticity and viscoplasticity into a unified set of equations suitable for multi-axial isotropic deformation. The model includes the effects of hydrostatic pressure, strain rate, and strain hardening which have been observed for thermoplastics in the glassy regime. The constitutive model is implemented into a finite element analysis program and appropriate parameters are identified for a polycarbonate. Capabilities of the model are demonstrated through the evaluation of a hard-body impact problem. © 2001 Elsevier Science Ltd. All rights reserved.

Keywords: Viscoelasticity; Plasticity; Structural polymers; Impact

1. Introduction

For structural applications, thermoplastics in the glassy range constitute the most commonly used form of polymers. One group of applications for which plastics are well suited is those requiring high impact resistance, including safety glass for windows and shower doors, windshields for automobiles and aircraft, and transparent armor. The primary reasons for this high impact resistance are high ductility, which allows structures made from these materials to undergo large deformation before failure, and nonlinear viscoelastic/viscoplastic (VE/VP) response, which allows the materials to transform a great deal of impact energy into heat or internal energy.

The same nonlinear VE/VP behavior that gives plastics good impact resistance also makes prediction of their response very difficult. To accurately represent the macroscopic mechanical response of polymeric structures subjected to impact loads, it is necessary to capture both the response at low levels of deformation (which typifies the condition of most of the structure) and the response at high levels of deformation (which typifies the condition of the structure in the immediate vicinity of the impact). At very low strains, plastics exhibit linear or nearly linear VE response. However, the range of strains for which linear viscoelasticity is an accurate approximation has been shown to be less than one percent for polymers such as

* Corresponding author. Tel.: +1-937-229-3018; fax: +1-937-229-4251.
E-mail address: frankgj@udri.udayton.edu (G.J. Frank).

0020-7683/01/$ - see front matter
PII: S0020-7683(00)00339-5

acrylic (Brüller and Schmidt, 1979) and polycarbonate (Frank, 1997). At higher strains, nonlinear viscoelasticity predominates, encompassing both a decreasing elastic modulus and an increasing relaxation rate with increasing deformation. Up to yield, which is taken as the upper maximum in a uniaxial tensile test, the stress is completely recoverable upon return to zero strain and allowing a suitable time for VE recovery (Frank, 1997). In the small to moderate deformation range, hydrostatic pressure has been shown to increase both the yield strength (Shimono et al., 1977) and the modulus (Gol'dman et al., 1989; Brown, 1986) of glassy polymers.

The yield point denotes the onset of permanent deformation. While a significant amount of literature has been generated regarding the apparent stress drop after yield in a tensile test, the true stress for most polymers in the glassy regime does not actually decrease after yield (G'Sell and Jonas, 1979, 1981). Rather, the formation of a traveling neck masks the actual pointwise stress response in the tensile specimen. The permanent deformation above yield is characterized by increasing stiffness at high elongation and the development of anisotropy due to molecular orientation. The molecular alignment increases both the flow resistance (Boyce et al., 1988a, b) and the small deformation modulus (Chudnovsky et al., 1994).

To simulate these behaviors requires a constitutive model that combines nonlinear VE effects with plasticity. Although there has been a great deal of research in both viscoelasticity and viscoplasticity, attempts to develop constitutive relations that combine the two areas have been limited. Landau et al., (1960) combined equations for a perfectly plastic solid obeying a temperature-dependent von Mises yield criterion with the relations of viscoelasticity developed from a single spring-dashpot model with nonconstant coefficients. Naghdi and Murch (1963) developed constitutive relations for linear VE/plastic behavior in which the VE strain rates are derived from the creep integral laws of linear viscoelasticity and the plastic strain rates are dependent on the time history of stress. Both of these theories decompose the strain rates into elastic, viscous, and plastic components. Ghoneim and Chen (1983) proposed constitutive relations that decompose the strains into VE and VP components. Elastic behavior is represented by a three-parameter solid of linear viscoelasticity, and plastic behavior uses isotropic hardening with a modified Drucker–Prager yield criterion (Prager, 1961). Vest et al., (1987) developed models for uniaxial, isothermal deformation based on extended mechanical analogies in which various types of elastic and inelastic elements are combined in series or parallel. These models provided good agreement which experimental data, but require that different combinations of elements be used to model different materials. Kitagawa et al., (1989) modified the Krempl's elastic/VP constitutive relations (Krempl, 1979) to include a three-parameter solid from linear viscoelasticity that has nonconstant coefficients. This model provided good agreement with experiment for monotonically increasing strains, but did not agree well for reversed strain histories (Kitagawa et al., 1989; Bordonaro and Krempl, 1991). More recently, Matsuoka (1992) used a theory of *molecular cooperativity* to combine linear viscoelasticity and plasticity relations in a form suitable for uniaxial deformation. These relations were able to predict a theoretic value for yield based solely on linear VE data.

Section 2 presents a VE/VP constitutive model that expands on the concept of molecular cooperativity to account for multi-axial loading, changes in loading rate, reversed loading, hydrostatic pressure effects, and strain hardening. Nonlinear viscoelasticity has been included by developing the VE portion of the equations under the general framework of irreversible thermodynamics presented by Schapery (1966, 1969, 1970). Although the new constitutive model captures most of the characteristics observed for glassy polymers, it is developed only for isotropic behavior and does not capture the development of anisotropy at high elongation.

2. Development of constitutive model

The theory of intermolecular cooperativity states that meshing between polymer chain segments, or *conformers*, limits the rate at which the segments can move under the influence of an externally applied

force. Certain types of motion can occur in small regions, or domains, and have a short relaxation time. Other types of motion require motion of a large domain of conformers and have a long relaxation time. The range of domain sizes leads to a distribution of relaxation times, which produces the rate dependence of the moduli and yield strengths observed for glassy polymers. Associated with each domain size is an ideal yield strength. This yield strength will only be achieved if the polymer medium is loaded at a rate that is high compared to the characteristic relaxation rate of that domain. In the model that follows, it is assumed that the yield strength for each domain has a distribution as a function of relaxation time that is similar to the distribution of shear moduli.

It must be noted that, although the model is based on a theory of conformal motion of polymer chains, not all of the functions are based on theoretical models of polymer behavior. Many of the functions used in the model were selected simply because they reproduce the response characteristics observed experimentally. Also, although the properties of polymers are generally strong functions of temperature, the equations have been presented only for isothermal conditions to simplify the notation. Note that implicit summation on repeated subscripts is assumed in the following equations, except for subscripts enclosed in parentheses. Subscripts in parentheses indicate a domain number and are not summed.

2.1. Decomposition of stress and strain rates

The distribution of domain sizes surrounding a particular point in a medium are assumed to be characterized by $N+1$ discrete ranges. Furthermore, the stress and strain states in the vicinity of a particular point are assumed to vary gradually enough that all sizes of domains about that point can be considered to have the same state.

The contribution of the kth domain to the Cauchy (true) stress, $\sigma_{ij(k)}$, is characterized as being separable into deviatoric (shear) and dilatational (bulk) components:

$$\sigma_{ij(k)} = \bar{\sigma}_{ij(k)} + p_{(k)}\delta_{ij} \tag{1}$$

where δ_{ij} is the Kronecker delta. The bulk component is the mean extensional stress:

$$p_{(k)} = \frac{1}{3}\left(\sigma_{11(k)} + \sigma_{22(k)} + \sigma_{33(k)}\right) \tag{2}$$

The total Cauchy stress at a point is the sum of the contributions from each of the $N+1$ domains:

$$\sigma_{ij} = \sum_{k=0}^{N} \sigma_{ij(k)} \tag{3}$$

The strain components ε_{ij} are separated into deviatoric and dilatational components:

$$\varepsilon_{ij} = \bar{\varepsilon}_{ij} + \tfrac{1}{3}e\delta_{ij} \tag{4}$$

The dilatation is:

$$e = \varepsilon_{11} + \varepsilon_{22} + \varepsilon_{33} \tag{5}$$

We assume that, at the domain level, the deviatoric portion of the strain rate, $\dot{\bar{\varepsilon}}_{ij}$, can be divided into VE and VP components:

$$\dot{\bar{\varepsilon}}_{ij} = \dot{\bar{\varepsilon}}^{\mathrm{ve}}_{ij} + \dot{\bar{\varepsilon}}^{\mathrm{p}}_{ij} \tag{6}$$

and that the dilatational portion of the strain rate, $\dot{e}$, is defined only by VE relations. Eq. (6) implies the total deviatoric strain rate, $\dot{\bar{\varepsilon}}_{ij(k)}$, is the same for each domain, even though the VE and VP components may be different.

2.2. Nonlinear viscoelasticity relations

For the kth domain the dilatational and deviatoric stress components are related to their respective strain components in a manner similar to the integral relations of linear viscoelasticity:

$$p_{(k)}(t) = \int_{-\infty}^{t} K_{(k)}[t'(t) - t'(\xi)] \frac{\partial e(\xi)}{\partial \xi} \mathrm{d}\xi \tag{7}$$

$$\bar{\sigma}_{ij(k)}(t) = 2 \int_{-\infty}^{t} G_{(k)}[t'(t) - t'(\xi)] \frac{\partial \bar{\varepsilon}^{\mathrm{ve}}_{ij(k)}}{\partial \xi} \mathrm{d}\xi \tag{8}$$

where $K_{(k)}(t)$ and $G_{(k)}(t)$ are bulk and shear relaxation moduli respectively. These moduli can be expressed as separable functions of stress and time:

$$K_{(k)}(t) = K_{(k)} \mathrm{e}^{-t/\tau_k} \tag{9}$$

$$G_{(k)}(t) = G_{(k)} g\left(J_{2(k)}, Z_{(k)}\right) \mathrm{e}^{-t/\tau_k} \tag{10}$$

$K_{(k)}$, $G_{(k)}$ and τ_k are constants experimentally defined by small-strain linear viscoelasticity, and the function $g(J_{2(k)}, Z_{(k)})$ permits the inclusion of the nonlinear VE effects observed at small to moderate strains. The form of $g(J_{2(k)}, Z_{(k)})$ has been chosen to represent the nonlinear softening noted at low to moderate stress levels in polymeric glasses:

$$g\left(J_{2(k)}, Z_{(k)}\right) = 1 - C_g \frac{3J_{2(k)}}{\left(Z_{(k)} + C_w W_{\mathrm{p}(k)}\right)^2} \tag{11}$$

$Z_{(k)}$ is the flow resistance of the material and $W_{\mathrm{p}(k)}$ is the plastic work done on this domain. The flow resistance and plastic work are defined in conjunction with the VP portion of this model. C_g and C_w are experimentally determined constants. C_g is less than one for materials that undergo strain hardening after yielding. $J_{2(k)}$ is the second invariant of the deviatoric stress, defined as:

$$J_{2(k)} = \tfrac{1}{2}\left(\bar{\sigma}_{ij}\bar{\sigma}_{ij}\right)_{(k)} \tag{12}$$

In Eq. (11), and in other equations presented later in this development, the quantity $3J_{2(k)}/\left(Z_{(k)} + C_w W_{\mathrm{p}(k)}\right)^2$ is used as a measure of the amount of recoverable deviatoric deformation in the kth domain. The exact amount of recoverable deviatoric deformation cannot be determined from the externally applied strain, since the strain at the domain level is continuously changing as the molecules realign themselves. However, the ratio of the total deviatoric stress in the kth domain (given by $3\sqrt{J_{2(k)}}$) to the current value of the yield strength (given by $Z_{(k)} + C_w W_{\mathrm{p}(k)}$) can be determined. This ratio provides an estimate of the recoverable deviatoric deformation. In Eq. (11) the yield strength includes an initial value, $Z_{(k)}$, and a term related to the plastic work, $C_w W_{\mathrm{p}(k)}$. The yield strength is allowed to vary linearly with plastic work to account for the increasing stiffness observed for glassy polymers at large elongation.

Nonlinearity in the relaxation function is introduced through a reduced time function developed from irreversible thermodynamic principles. In general the reduced time t' can be defined as a general function of stress and strain:

$$t' = \int_0^t \frac{\mathrm{d}\tau}{\phi(\sigma, \varepsilon)} \tag{13}$$

A thermodynamically admissible time shift requires that $\phi(\sigma, \varepsilon) \geqslant 0$ (Schapery, 1970).

For this model, the Doolittle relation for free volume is used for the shift function. The Doolittle relation previously was used for a shift function by Knauss and Emri (1981, 1987) and by Shay and Caruthers

(1987). This relation provided reasonable simulation of strain softening behavior for loading in tension and has the form:

$$\phi_{(k)} = \exp\left[b\left(\frac{1}{f_{(k)}(t)} - \frac{1}{f_0}\right)\right] \tag{14}$$

where the Doolittle constant, b, and the initial free volume, f_0, are experimentally determined. Because the free volume $f(t)$ was previously related to dilatational strain or to pressure and specific volume, the shift function of Eq. (14) did not provide agreement with experimental data for loading in compression. In this work, the free volume is defined as a function of the portion of the deviatoric stress in each domain:

$$f_{(k)}(t) = f_0 + C_v \frac{3J_{2(k)}}{\left(Z_{(k)} + C_w W_{\mathrm{p}(k)}\right)^2} \tag{15}$$

where C_v is an experimentally determined constant. The ratio of $J_{2(k)}$ to $\left(Z_{(k)} + C_w W_{\mathrm{p}(k)}\right)^2$ has again been used to approximate the amount of recoverable deviatoric deformation in the kth domain.

2.3. Viscoplasticity relations

This model assumes that there is an ideal yield strength associated with each domain size. If the deformation rate is low compared to the relaxation rate associated with the domain size, viscoelasticity will allow the conformers to reorient themselves without plastic deformation. However, if the deformation rate is sufficiently high compared to the relaxation rate, the stress may exceed the yield strength before significant viscous relaxation occurs.

To define the onset of plastic deformation, the relations developed by Bodner and Partom (1972, 1975) are used. These relations were based on the dynamics of dislocations in metals and do not have an underlying theoretical basis in terms of deformation mechanisms in polymeric materials. Since the molecular mechanisms associated with permanent deformation in glassy polymers are not currently well understood, the Bodner–Partom model is used with some modifications.

The original Bodner–Partom model has been modified to account for the effects of pressure on yield and to permit monotonically increasing resistance to flow with increasing deformation. The form of the equations presented here allows the onset of plasticity to be made nearly rate independent by an appropriate selection of constants. This nearly rate-independent form differs from the original formulations of Bodner and Partom and has been selected because the VE portion of the model controls the rate effects on yield.

In this model, as in many other plasticity relations, it is assumed that the plastic portion of the deviatoric strain rate is proportional to the deviatoric stress:

$$\bar{\dot{\varepsilon}}^{\mathrm{p}}_{ij(k)} = \lambda_{(k)} \bar{\sigma}_{ij(k)} \tag{16}$$

The factor of proportionality $\lambda_{(k)}$ is defined in terms of the second invariant of the deviatoric stress, $J_{2(k)}$ and the flow resistance, $Z_{(k)}$:

$$\lambda_{(k)} = \frac{D_0}{\sqrt{J_{2(k)}}} \left(\frac{3J_{2(k)}}{\left(Z_{(k)}\right)^2}\right)^n \tag{17}$$

where D_0 is the limiting VP deformation rate and n is an experimentally determined constant. High values of n (on the order of 1000 or more) provide nearly rate-independent plasticity (with the rate-dependence of the yield resulting in this model from VE effects).

To maintain stability in the integration of the equations, the practical restriction that the plastic deformation rate does not exceed the total deformation rate is imposed:

$$\dot{\bar{\varepsilon}}^{\mathrm{p}}_{ij(k)}\dot{\bar{\varepsilon}}^{\mathrm{p}}_{ij(k)} \leqslant \dot{\bar{\varepsilon}}_{mn}\dot{\bar{\varepsilon}}_{mn} \tag{18}$$

If the plastic strain rate predicted by Eqs. (16) and (17) violates Eq. (18), $\lambda_{(k)}$ is scaled to produce equality in Eq. (18). It should be noted that numeric instabilities have occurred in some implementations of Bodner–Partom plasticity models (Rajendran and Grove, 1987). Imposing Eq. (18) eliminates these instabilities.

To accommodate the effects of pressure observed for glassy polymers, the flow resistance is related to a pressure-free flow resistance $Z'_{(k)}$ and the pressure, $p_{(k)}$:

$$Z_{(k)} = Z'_{(k)}e^{-p_{(k)}/P_{0(k)}} \tag{19}$$

The pressure sensitivity factor P_0 is assumed to have a distribution with respect to relaxation time similar to that of the bulk modulus. Thus, $P_{0(k)}$ can be expressed as:

$$P_{0(k)} = P_0\frac{K_{(k)}}{\sum_{i=0}^{N}K_i} \tag{20}$$

where P_0 is an experimentally identified constant.

The pressure-free flow resistance, $Z'_{(k)}$, increases as a function of the plastic work rate, $\dot{W}_{\mathrm{p}(k)}$, and the current value of the flow resistance. This increase is defined in terms of a first order differential equation which provides a monotonically increasing function, simulating the increase in flow resistance which occurs for glassy polymers at high elongation. The particular form is:

$$\dot{Z}'_{(k)}(t) = m\left(\frac{Z'_{(k)}(t) - (1-\alpha)Z_{0(k)}}{Z_{0(k)}}\right)\dot{W}_{\mathrm{p}(k)} \tag{21}$$

where m, α, and $Z_{0(k)}$ are constants. $Z_{0(k)}$ is the initial value of the pressure-free flow resistance, m defines the rate of increase of the flow resistance, and α is related to the strain at which flow resistance begins to increase. The rate of plastic work is given by:

$$\dot{W}_{\mathrm{p}} = \sigma_{ij}\dot{\bar{\varepsilon}}^{\mathrm{p}}_{ij} \tag{22}$$

In accordance with the theory of molecular cooperativity, it is assumed that the yield strength has a distribution with respect to relaxation time that is similar to the distribution of the shear modulus. Thus, $Z_{0(k)}$ can be expressed as:

$$Z_{0(k)} = Z_0\frac{G_{(k)}}{\sum_{i=0}^{N}G_i} \tag{23}$$

where Z_0 is an experimentally determined constant.

2.4. Incremental form of the constitutive equations

The integral equations used in the material model described above must be evaluated using numeric integration. The most practical use for this model is in a finite element analysis program that uses explicit integration for propagating the solution forward in time. Most codes of this type use velocities at a grid of node points as the primary unknowns in the solution. The material models use the strain rates as the basis for calculating point stresses. This form of the material model is said to be *strain driven*, since the deformations are treated as known quantities in the calculation of the stresses. The strain-driven point stress problem is: given the material state $\left(p, \bar{\sigma}_{ij}, e, \bar{\varepsilon}_{ij}, \text{etc.}\right)$ at time t, and deformation rates $\dot{e}$, $\dot{\bar{\varepsilon}}_{ij}$ for a time interval from t to $(t+\Delta t)$, determine the material state at time $(t+\Delta t)$.

For the material model described above, both the dilatational and deviatoric components of stress are derived from hereditary integrals. That is, the computation of stress at a time t requires the strain history for the time interval $(-\infty, t]$. For a finite element analysis (FEA) program that uses explicit integration techniques, the strain rates are constant within a time step. Following a procedure outlined by Brockman (1990), constant strain rates within a time step allow the hereditary integrals to be recast in a rate form which eliminates the need to store strain histories at the stress sampling points. Substituting from Eqs. (9) and (10) into Eqs. (7) and (8) for $K_{(k)}(t)$ and $G_{(k)}(t)$ and performing some algebraic manipulations gives the pressure and deviatoric stress on each domain at time $(t + \Delta t)$ as:

$$p_{(k)}(t+\Delta t) = \mathrm{e}^{-\alpha_{(k)}/\tau_k}\left[p_{(k)}(t) + K_{(k)}\dot{e}\int_t^{t+\Delta t} \exp\big(-\big[t'(t) - t'(\xi)\big]/\tau_k\big)\,\mathrm{d}\xi\right] \tag{24}$$

$$\bar{\sigma}_{ij(k)}(t+\Delta t) = \mathrm{e}^{-\alpha_{(k)}/\tau_k}\left[\bar{\sigma}_{ij(k)}(t) + 2G_{(k)}\bar{\dot{\varepsilon}}^{\mathrm{ve}}_{ij(k)}\int_t^{t+\Delta t} g\big(J_{2(k)}, Z_{(k)}\big)\exp\big(-\big[t'(t) - t'(\xi)\big]/\tau_k\big)\,\mathrm{d}\xi\right] \tag{25}$$

For simplifying the notation, $1/\tau_0 = 0$ is used in the preceding two equations. The value of $\alpha_{(k)}$ is computed as:

$$\alpha_{(k)} = \int_t^{t+\Delta t} \exp\big(b\big[1/f_0 - 1/f_{(k)}(u)\big]\big)\,\mathrm{d}u \tag{26}$$

Since the strain rates are constant within a time step, the integrals that appear in Eqs. (24)–(26) can be computed using low-order Gaussian quadrature rules, and $p_{(k)}$ and $\bar{\sigma}_{ij(k)}$ form a set of $7(N+1)$ state variables that must be stored and updated for each material point. The complete stress tensor at each material point is simply summed from the contributions of each domain:

$$\sigma_{ij}(t+\Delta t) = \sum_{k=0}^{N}\Big[\bar{\sigma}_{ij(k)}(t+\Delta t) + \delta_{ij}p_{(k)}(t+\Delta t)\Big] \tag{27}$$

2.5. Specialized forms of the constitutive equations

The constitutive equations presented above include, as special cases, several traditional constitutive models. These traditional models are obtained by appropriate selection of constants in the model described above. Some of the models that can be obtained are listed in Table 1.

3. Model parameters for polycarbonate

The large number of parameters in the VE/VP constitutive model complicates the determination of appropriate parameters for use with different materials. For identifying constitutive model parameters from experimental data, a method has been developed that uses nonlinear optimization techniques (Frank, 1998). The optimization minimizes an objective function which is formed from the square of the difference between measured and simulated stress response for various types of simple mechanical property tests, such as uniaxial tension or compression, biaxial loading, torsion loading, etc. For simulating the tests, a procedure has been developed that uses a one-dimensional search algorithm to establish strain rate components that satisfy the field equations of continuum mechanics.

Table 2 presents parameters for polycarbonate at 22°C based on experimental data collected for a single resin (Frank, 1997). The parameters were identified based on measured data from uniaxial tension, uniaxial

Table 1
Specialized constitutive models obtainable from VE/VP model

Parameter	Units	Linear elastic model	Linear VE model	Linear elastic model with rate dependent yield
N	–	0	V	0
G_0	FL^{-2}	V	V	V
G_i $(i = 1, 2, \ldots, N)$	FL^{-2}	N/A	V	N/A
K_0	FL^{-2}	V	V	V
K_i $(i = 1, 2, \ldots, N)$	FL^{-2}	N/A	V	N/A
τ_i $(i = 1, 2, \ldots, N)$	T	N/A	V	N/A
C_g	–	0	0	0
C_w	–	0	0	0
f_0	–	1	1	1
b	–	1	1	1
C_v	–	0	0	0
D_0	T^{-1}	1×10^{11}	1×10^{11}	V
n	–	1×10^{3}	1×10^{3}	V
m	–	0	0	V
α	–	0	0	V
Z_0	FL^{-2}	1×10^{12}	1×10^{12}	V
P_0	FL^{-2}	1×10^{12}	1×10^{12}	1×10^{12}

V-indicates that the value of the parameter must be determined from experimental data. N/A-indicates a parameter that is not used when $N = 0$. Designations for units: F = force, T = time, L = length.

Table 2
Constitutive model parameters for polycarbonate at 22°C

Miscellaneous constants		Shear moduli (Pa)		Bulk moduli (Pa)		Time constants (s)	
D_0	1.00E+11	G_0	5.81E+08	K_0	1.64E+09		
n	1.00E+03	G_1	2.31E+07	K_1	1.57E+08	τ_1	1.0E+08
m	5.00E+01	G_2	2.68E+07	K_2	1.72E+08	τ_2	1.3E+07
α	9.14E−06	G_3	2.91E+07	K_3	1.78E+08	τ_3	1.6E+06
Z_0	1.86E+08	G_4	2.79E+07	K_4	1.62E+08	τ_4	2.0E+05
P_0	9.14E+08	G_5	2.70E+07	K_5	1.49E+08	τ_5	2.5E+04
C_g	9.90E−01	G_6	2.97E+07	K_6	1.55E+08	τ_6	3.2E+03
C_w	1.25E−01	G_7	3.28E+07	K_7	1.63E+08	τ_7	4.0E+02
f_0	2.00E−01	G_8	3.24E+07	K_8	1.53E+08	τ_8	5.0E+01
b	2.64E+00	G_9	3.04E+07	K_9	1.36E+08	τ_9	6.3E+00
C_v	3.01E−01	G_{10}	3.01E+07	K_{10}	1.28E+08	τ_{10}	8.0E−01
N	24	G_{11}	3.12E+07	K_{11}	1.26E+08	τ_{11}	1.0E−01
		G_{12}	3.28E+07	K_{12}	1.26E+08	τ_{12}	1.3E−02
		G_{13}	3.47E+07	K_{13}	1.26E+08	τ_{13}	1.6E−03
		G_{14}	3.75E+07	K_{14}	1.30E+08	τ_{14}	2.0E−04
		G_{15}	4.18E+07	K_{15}	1.37E+08	τ_{15}	2.5E−05
		G_{16}	4.79E+07	K_{16}	1.50E+08	τ_{16}	3.2E−06
		G_{17}	5.64E+07	K_{17}	1.67E+08	τ_{17}	4.0E−07
		G_{18}	6.78E+07	K_{18}	1.91E+08	τ_{18}	5.0E−08
		G_{19}	8.20E+07	K_{19}	2.19E+08	τ_{19}	6.3E−09
		G_{20}	9.76E+07	K_{20}	2.47E+08	τ_{20}	8.0E−10
		G_{21}	1.13E+08	K_{21}	2.70E+08	τ_{21}	1.0E−10
		G_{22}	1.26E+08	K_{22}	2.87E+08	τ_{22}	1.3E−11
		G_{23}	1.38E+08	K_{23}	2.97E+08	τ_{23}	1.6E−12
		G_{24}	1.46E+08	K_{24}	2.98E+08	τ_{24}	2.0E−13

compression, bulk modulus, creep, and resonant beam tests. Figs. 1–5 compare measured data and response predicted by the VE/VP model for a variety of uniaxial loading conditions.

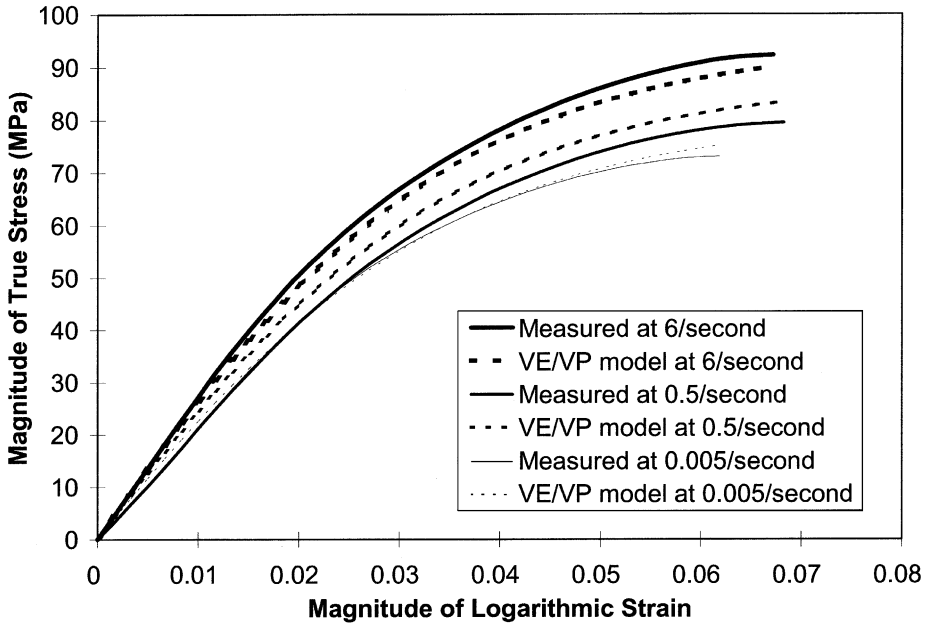

Fig. 1. Predicted and measured response in compression tests to yield.

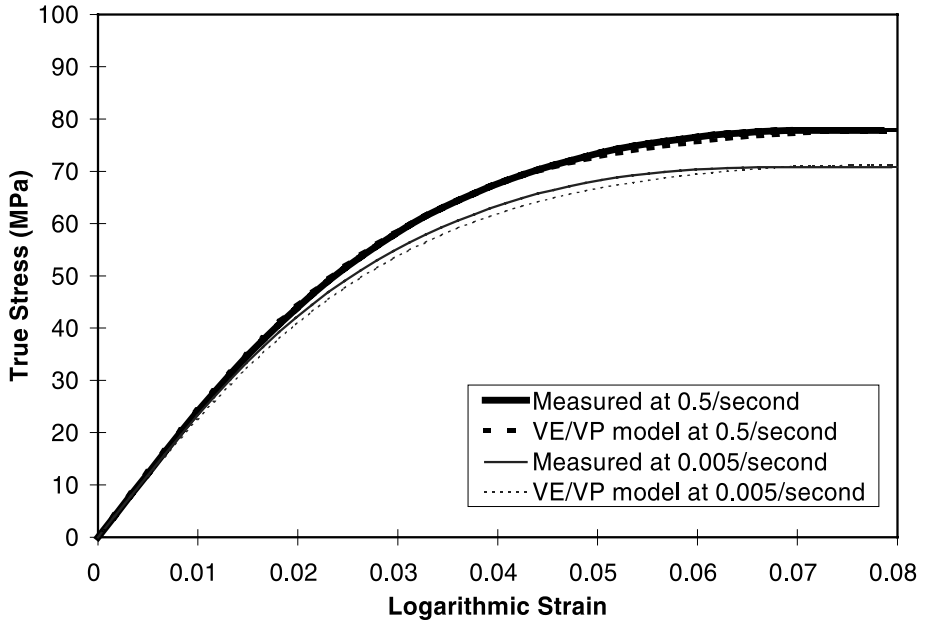

Fig. 2. Predicted and measured response during initial portion of tension tests.

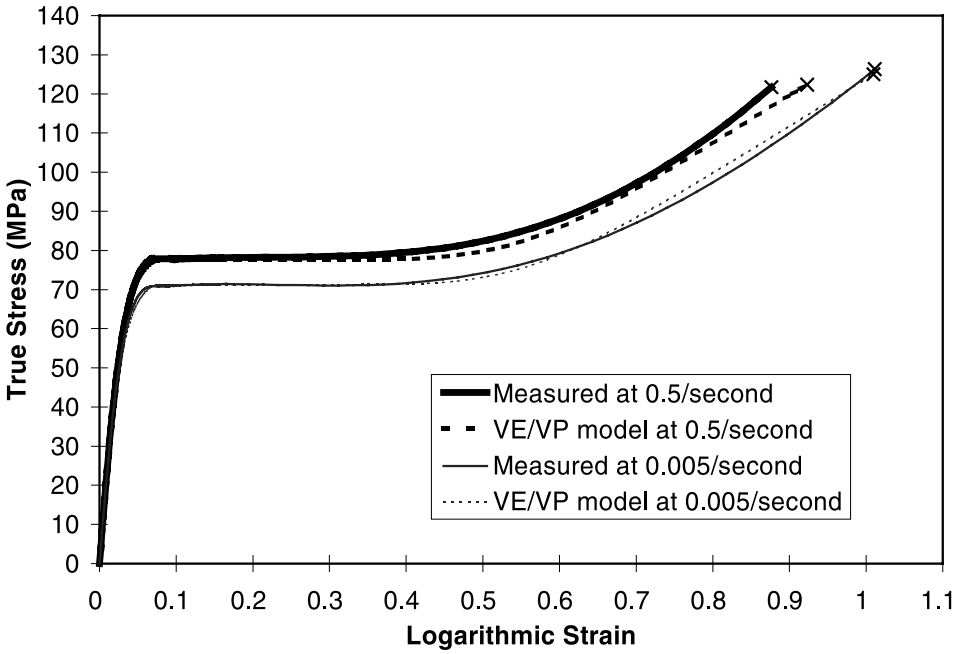

Fig. 3. Predicted and measured response during tension tests to failure.

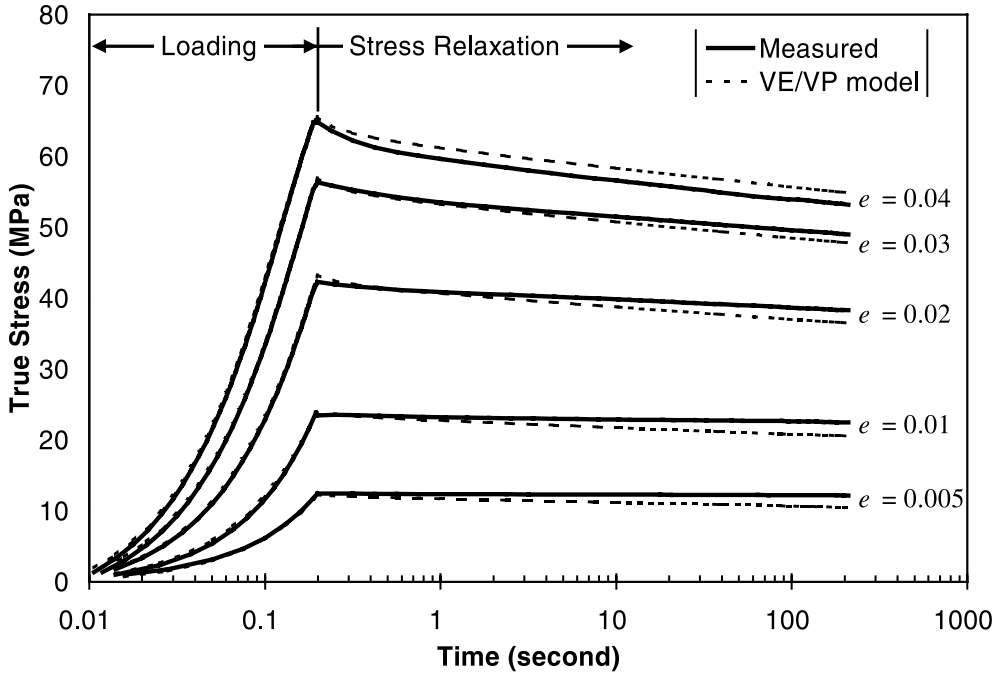

Fig. 4. Response during stress relaxation at several strain levels.

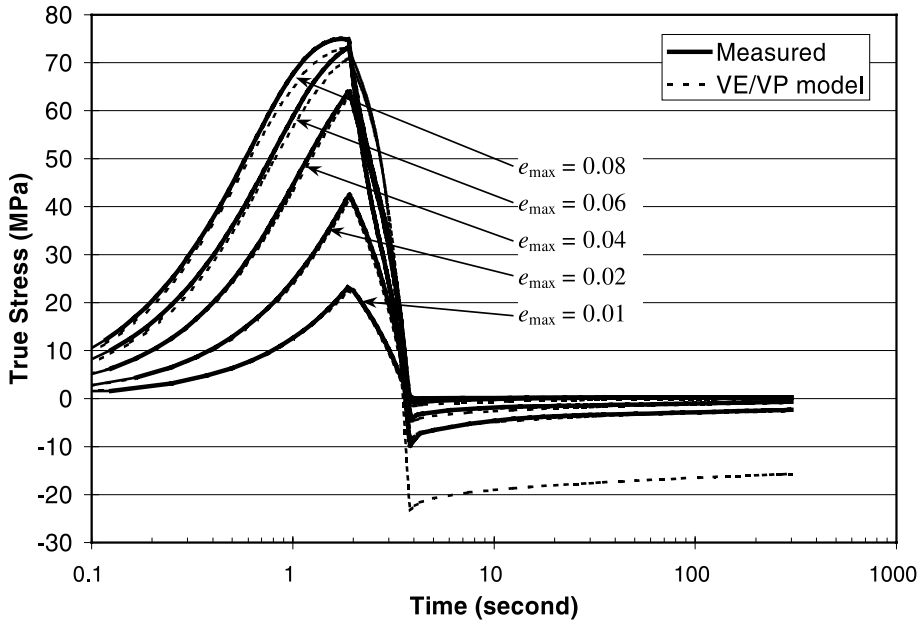

Fig. 5. Response during a series of single-cycle tests with strain held at zero after conclusion of loading.

Fig. 1 shows measured and predicted responses during compression tests at three rates to the yield point, where compressive stresses and strains are shown as positive quantities. The predicted data follows the measured trend of increasing stiffness with increasing loading rate. Data is shown only to yield, since beyond yield the compression specimens are prone to failure by buckling.

Fig. 2 shows measured and predicted responses during tensile tests at two rates to an axial strain of 0.08. Fig. 3 shows similar data to failure. The figures show good agreement between experimental and predicted data for monotonic tensile loading. It should be noted that the "measured" stress–strain behavior in Fig. 3 above a strain of 0.08 was estimated based on the measured yield and failure points and the response known to produce necking under a monotonically increasing tensile load at a constant strain rate.

Fig. 4 shows the stress during a series of stress relaxation tests at five different strain levels. Fig. 4 shows good agreement between measured and predicted response during the loading portion of the tests. During relaxation, the model overpredicts the relaxation rate at very low strains and underpredicts the relaxation rate at high strains, but overall agreement between measured and predicted responses is good. It should be mentioned that, in the property identification procedure, greater weight has been given to response during loading, since our primary interest is in applications of the model to impact analysis.

Fig. 5 shows the stress during a series of five cyclic tests. In these tests the axial strain was ramped at a constant rate to the value indicated as e_{max}, ramped back to zero at the same rate, and held at zero while the stress relaxed. Fig. 5 shows good agreement between measured and predicted response during the loading portion of the test and during the relaxation portion of the tests (4 s and beyond) for tests with a maximum strain up to 0.06 in./in. The relatively poor agreement observed for the test with a maximum strain of 0.08 in./in. is due to the prediction of permanent deformation by the VE/VP model at a lower strain than that which actually induces permanent deformation. Because the model parameters are selected to provide good agreement with the test data for large plastic deformations (Fig. 3), a minor degree of inaccuracy in the neighborhood of the initial yield point is not unexpected.

4. Example application

The VE/VP constitutive model has been implemented in the finite element analysis code X3D (Brockman and Held, 1992), and simulations of simple structures undergoing loading at high rates have been performed. In this section, results are presented for one case that demonstrates some practical aspects of the model. This analysis uses the parameters for polycarbonate described above.

A standard test method, ASTM D 3029, for determining the impact resistance of plastics is by impacting them with a falling dart. Determination of the energy (mass of dart times height from which it is dropped) required to break flat plastic sheets of a specific geometry can be used to rank the plastics. Typically polycarbonate specimens, if they do not break, have a large protrusion indicative of significant plastic deformation. In this verification case, the deformed shape of a polycarbonate specimen that did not break after being impacted is compared with FEA predictions.

The configuration used for the testing is illustrated in Fig. 6. The 13.2 mm thick polycarbonate coupon was impacted by an 18.1 kg dart, dropped from 6.1 m (Frank and Stenger, 1992). Measurements of the profile of the deformed specimen were made approximately seven days after the test.

The impact test has been simulated by FEA with both the VE/VP constitutive model and a bilinear elastic/plastic (E/P) constitutive model with rate-dependent yield (Brockman and Held, 1992). Parameters used for the E/P model have been used previously for impact analysis (Huelsman et al., 1994).

The response of the plate during the impact is illustrated in Fig. 7. Immediately after the dart impacts the coupon at 10.9 m/s, the center begins to form a cavity, and the corners lift off the supporting rim. The FEA indicates that at 5.5 ms after impact, the maximum deflection is achieved and the dart begins to rebound. At 9.5 ms after impact, the dart separates from contact with the plate. At approximately the same time, the plate separates from contact with the support rail. In the actual test the dart is caught before it can impact the plate a second time. After the dart leaves the surface of the plate in the FEA analysis, the dart is restrained from motion and dynamic relaxation is used to suppress the free vibrations of the plate. For the FEA simulation that uses the E/P material model, the residual stresses are in equilibrium after dynamic relaxation. For the FEA simulation using the VE/VP constitutive model, the residual stresses are not in equilibrium after dynamic relaxation due to VE relaxation which is included in the VE/VP constitutive model. Continuing the FEA simulation with the VE/VP constitutive model for an additional 4 ms after all free vibration has stopped allows the determination of the rate at which the deformed shape is changing due to VE relaxation.

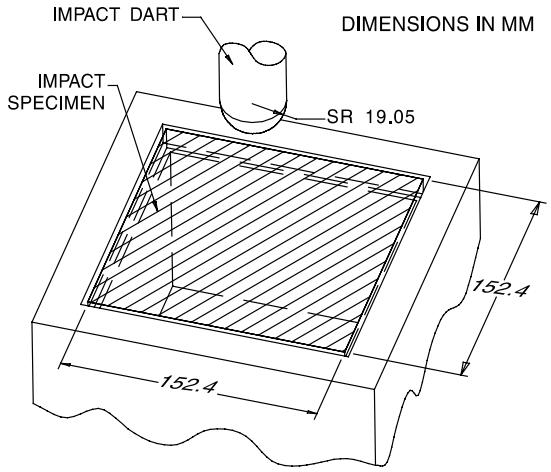

Fig. 6. Conditions for falling dart impact test.

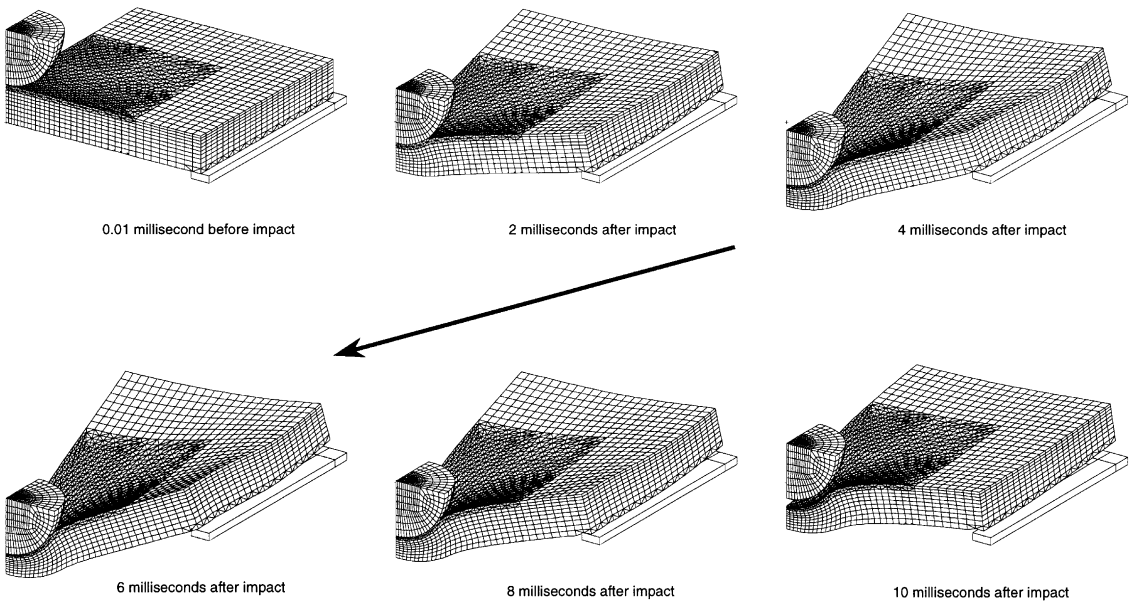

Fig. 7. Deformations at intervals during falling dart impact test.

The solid diamonds in Fig. 8 shows the shape of the coupon measured approximately seven days after the impact test was performed. The measured points lie on a line that runs from the mid-side of one edge to the mid-side of the opposing edge.

The hollow squares in Fig. 8 indicate the deformed shape predicted by FEA with the E/P constitutive model, which overpredicts the permanent deformation of the panel. We should emphasize that this is not necessarily typical: in numerous impact analyses of acrylic and polycarbonate parts, we have observed E/P results that are both too compliant and too stiff. The only clear trend is that the E/P model, even with rate corrections, does not provide reliable predictions. The hollow triangles in Fig. 8 show the deformed shape predicted by FEA with the VE/VP constitutive model at the end of the simulation, 18 ms after impact. The measured data, taken approximately one week after the experiment, suggest that a substantial amount of creep occurs following the impact. The VE/VP constitutive model is capable of predicting the shape change with time due to VE relaxation, by continuing the calculation for a short time after the loading event is concluded. Most relaxation and creep phenomena occur on a logarithmic time scale. Thus, to a first approximation, the position of points on the panel at time T_{final} can be extrapolated from the FEA predictions at 14 and 18 ms as:

$$\mathbf{x}_{T_{\text{final}}} \approx \mathbf{x}_{0.014\ \text{s}} + \frac{(\mathbf{x}_{0.018\ \text{s}} - \mathbf{x}_{0.014\ \text{s}})}{\log(0.018\ \text{s}) - \log(0.014\ \text{s})}(\log(T_{\text{final}}) - \log(0.014\ \text{s}))$$

Extrapolating to $T_{\text{final}} = 7$ days produces the predicted shape shown by the hollow circles. [1] Considering the simplicity of the method used for extrapolation, the measured data and the extrapolated FEA solution show remarkably good agreement.

[1] The precise time elapsed between the impact test and the profile measurements was not recorded. However, on the logarithmic time scale, altering T_{final} even by a few days either way does not produce a noticeable change in the final shape extrapolated from the 14 and 18 ms data.

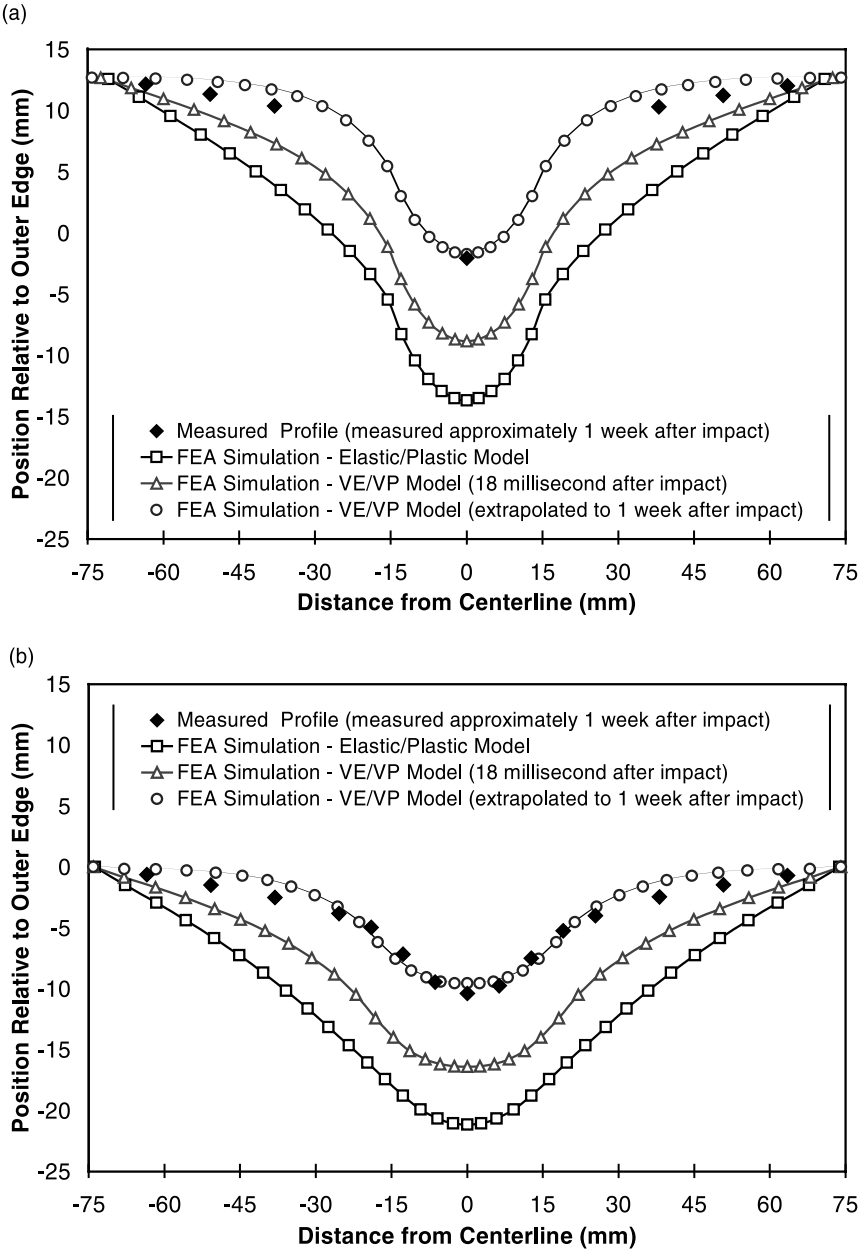

Fig. 8. Deformed shape of polycarbonate plate after impact by 18.1-kg falling dart: (a) concave (upper) surface, (b) convex (lower) surface.

5. Summary and conclusions

This work develops a unified set of constitutive equations that combine nonlinear viscoelasticity and viscoplasticity and captures most of the time-dependent, nonlinear response observed for glassy polymers,

including: rate-dependent and pressure-dependent modulus and yield; decreasing modulus and increasing relaxation rate with increasing deformation; permanent deformation beyond yield; and strain hardening at high elongation. To the best of our knowledge, this is the first time nonlinear viscoelasticity and plasticity have been combined in a form suitable for multi-axial response. The model includes as special cases several traditional types of constitutive equations, including linear elasticity, linear viscoelasticity, and plasticity with or without strain hardening.

In forming this constitutive model, several empirical relationships are used that represent the response observed for glassy polymers under many types of loading. The use of these empirical relationships has allowed this development to avoid some of the limitations of more theoretical developments that represent observed response only for a limited range of conditions. To ascertain the validity of the assumptions used in developing this model, further research is required into the basic mechanics of polymer deformation.

Inclusion of anisotropic behavior in the VE/VP constitutive model would improve correlation with observed behavior in some regimes. The effect of anisotropy on the plastic flow due to chain orientation could be included by incorporating a tensorial form of the flow resistance that has been used in VP relations for metals (Bodner, 1991; Stouffer and Bodner, 1979). The link between effective deviatoric stress and effective yield strength in the VE/VP model would produce a secondary result of increasing the stiffness in the direction of molecular orientation, an effect which has been noted for some glassy polymers.

Acknowledgements

Financial support for this work was provided by the Flight Dynamics Directorate of the Air Force Wright Laboratory Wright–Patterson Air Force Base, Ohio, under Air Force contract F33615-92-C-3400. Additional support was provided by a grant of computer time from the Department of Defense High Performance Computing Center, Major Shared Resource Center, SGI Power Challenge Array.

References

Bodner, S.R., 1991. In: Freed, A.D., Walker, K.P. (Eds.), High Temperature Constitutive Modeling – Theory and Application, vol. MD-26, ASME Materials Division, Atlanta, Georgia, pp. 175–184.

Bodner, S.R., Partom, Y., 1972. J. Appl. Mech. 39, 751–757.

Bodner, S.R., Partom, Y., 1975. J. Appl. Mech. 42, 385–389.

Bordonaro, C.M., Krempl, E., 1991. Proc. Winter Annual Meeting of the American Society of Mechanical Engineers, vol. 29. ASME, Materials Division, Atlanta, Georgia, p. 33–45.

Boyce, M.C., Parks, D.M., Argon, A.S., 1988a. Mech. Mater. 7, 15–33.

Boyce, M.C., Weber, G.G., Parks, D.M., 1988b. J. Mech. Phys. Solids 37, 647–665.

Brockman, R.A., 1990. A Nonlinear Viscoelastic Material Model with Pressure Ageing. Report UDR-TR-90-12, University of Dayton Research Institute, Dayton, Ohio.

Brockman, R.A., Held, T.W., 1992. X3D User's Manual. Report UDR-TR-92-59, University of Dayton Research Institute, Dayton, Ohio.

Brown, N., 1986. In: Brostow, W., Corneliussen, R.D. (Eds.), Failure of Plastics. Hanser Publishers, Munich, pp. 98–118.

Brüller, O.S., Schmidt, H.H., 1979. Poly. Eng. Sci. 19, 883–887.

Chudnovsky, A., Chen, T.J., Zhou, Z., Bosnyak, C.P., Sehanobish, K., 1994. Failure Analysis for Polycarbonate Transparencies. WL-TR-94-3064, Wright Laboratory, Air Force Materiel Command, Wright–Patterson AFB, Ohio.

Frank, G.J., 1997. Analytic and Experimental Evaluation of the Effects of Temperature and Strain Rate on the Mechanical Response of Polymers. Report UDR-TR-97-152, University of Dayton Research Institute, Dayton, Ohio.

Frank, G.J., 1998. A Constitutive Model for the Mechanical Response of Glassy Polymers. Ph.D. Thesis, University of Dayton, Dayton, Ohio.

Frank, G.J., Stenger, G.J., 1992. Frameless Transparency System Material Property Evaluation. Report UDR-TR-92-51, University of Dayton Research Institute, Dayton, Ohio.

Ghoneim, H., Chen, Y., 1983. Comp. Struct. 17, 499–509.
Gol'dman, A.Y., Demenchuk, N.P., Murzakhanov, G.K., 1989. Mech. Comp. Mat. 24, 707–714.
G'Sell, C., Jonas, J.J., 1979. J. Mat. Sci. 14, 583–591.
G'Sell, C., Jonas, J.J., 1981. J. Mat. Sci. 16, 1956–1974.
Huelsman, M.A., Roach, K.P., Frank, G.J., Braisted, W.R., 1994. Effect of Melt Flow Index on the Impact Resistance, Dimensional Variation, and Mechanical Properties of Injection Molded Polycarbonate. Report WL-TR-94-3040, Air Force Materiel Command, Wright Patterson AFB, Ohio.
Kitagawa, M., Mori, T., Matsutani, T., 1989. J. Poly. Sci.: Part B: Poly. Phys. 27, 85–95.
Knauss, W.G., Emri, I., 1981. Comp. Struct. 13, 123–128.
Knauss, W.G., Emri, I., 1987. Poly. Engng. Sci. 27, 86–100.
Krempl, E., 1979. J. Engng. Mat. Tech. 101, 380.
Landau, H.G., Weiner, J.H., Zwicky, E.E. Jr., 1960. J. Appl. Mech. 27, 297–302.
Matsuoka, S., 1992. Relaxation Phenomena in Polymers. Hanser Publishers, Munich.
Naghdi, P.M., Murch, S.A., 1963. J. Appl. Mech. 30, 321–328.
Prager, W., 1961. Introduction to Mechanics of Continuous Media. Ginn and Co, Boston.
Rajendran, A.M., Grove, D.J., 1987. Bodner–Partom Viscoplasticity Model in STEALTH Finite Difference Code. Report AFWAL-TR-86-4098, Materials Laboratory, Air Force Wright Aeronautical Laboratories, Wright Patterson AFB, Ohio.
Schapery, R.A., 1966. Int. J. Solids Struct. 2, 407–425.
Schapery, R.A., 1969. Poly. Engng. Sci. 9, 295–310.
Schapery, R.A., 1970. In: Boley, B.A. (Ed.), Thermoinelasticity (IUTAM Symposium on Thermoinelasticity, 1968). Springer, New York, pp. 259–285.
Shay, R.M.J., Caruthers, J.M., 1987. Developments in Mechanics, Proc. 20th Midwestern Mechanics Conference, vol. 14(b). Purdue University, West Lafayette, Indiana, pp. 493–498.
Shimono, M., Nakayama, T., Inoue, N., 1977. 20th Japan Congress on Materials Research – Nonmetallic Materials, pp. 220–225.
Stouffer, D.C., Bodner, S.R., 1979. Int. J. Engng. Sci. 27, 757.
Vest, T.A., Amoedo, J., Lee, D., 1987. vol. 85. In: Stokes, V.K., Krajcinovic, D. (Eds.), Constitutive Modeling for Nontraditional Materials, ASME, Applied Mechanics Division, Boston, Massachusetts, pp. 71–86.